Electronic Supplementary Material (ESI) for Inorganic Chemistry Frontiers.

Supporting Information

Regulating Spin Density of Co^{III} by Boron-doped Carbon Dots for Enhanced Electrocatalytic Nitrate Reduction

Jingjing Huang,† Jingkun Yu,† Xingmei Lu, Yingying Wei, Haoqiang Song, Ang Cao, Jinmeng Cai, Shuang-Quan Zang and Siyu Lu**

Experimental section

Chemical and materials

3-aminobenzene borate hydrochloride ($C_6H_9BClNO_2$), ammonium chloride ($^{14}NH_4Cl$, $^{15}NH_4Cl$), concentrated sulfuric acid (H_2SO_4), anhydrous ethanol (C_2H_6O), ultra-pure water (H_2O), potassium sulfate (K_2SO_4), potassium nitrate ($K^{14}NO_3$, $K^{15}NO_3$), Maleic acid ($C_4H_4O_4$), $CoCl_2{\cdot}6H_2O$, D_2O and Urea (CH_4N_2O) were purchased from Aladdin (Shanghai, China). All reagents have not been purified before use.

Preparation of the electrocatalysts

The preparation process of BCDs is to dissolve $C_6H_9BClNO_2$ (1 mmol) in deionized water (10 mL), mix it evenly, and keep it under 200 °C in hydrothermal condition for 8 h. 3.2 mmol $CoCl_2{\cdot}6H_2O$, 0.3 g BCDs and 15 mmol urea were added into 30 mL of ultra-pure water and stirred for 30 min. The mixed solution was transferred to a 50 mL Teflon-lined stainless steel autoclave, and a clean carbon cloth (CC) (3 × 2 cm^2) was placed into the autoclave. The reaction was heated to 120 ℃ for 6 h. After the reaction, the autoclave was cooled to room temperature. The CC was alternately rinsed with ultra-pure water and ethanol (3 times). The catalyst precursor of BCDs/$Co(OH)_x$/CC was then dried in a vacuum oven at 60 ℃. Finally, the catalyst precursor of BCDs/$Co(OH)_x$/CC was calcined in air at 450 ℃ for 2 h to obtain BCDs@Co_3O_4/CC.

Characterization

Scanning electron microscopy (SEM) images were taken on a Hitachi S-4800 scanning electron microscope (3 kV). Transmission electron microscopy (TEM) images and higher-resolution transmission electron microscopy (HRTEM) images were obtained with a Tecnai G2 F20 system equipped with energy dispersive analysis of X-rays (EDAX) capabilities. X-ray diffraction (XRD) patterns were recorded on a Bruker D8 Focus Diffraction System using a Cu Kα source (λ = 0.15406 nm). X-ray photoelectron spectroscopy (XPS) measurements were performed on a 5000 VersaProbe (PHI) instrument using Al Kα radiation as the excitation source. All spectra were calibrated using the C 1s signal at 284.6 eV due to adventitious hydrocarbons.

^{15}N isotope labeling experiments

The aforementioned electrochemical nitrate reduction method was used for the isotopically labelled nitrate reduction experiments, except that the nitrogen source was changed to 99.0 atom% $K^{15}NO_3$. Using a ^1H NMR method (Bruker 600-MHz system), the amounts of $^{15}NH_4^+$

and $^{14}NH_4^+$ in the electrolyte after the reaction could be qualitatively and quantitatively measured. Taking $^{15}NH_4^+$ as an example, the specific steps were as follows: Firstly, a series of 0.5 M K_2SO_4 solutions with specific concentrations of $(^{15}NH_4)_2SO_4$ were prepared as standard solutions. Next, the external standard maleic acid ($C_4H_4O_4$) was added to each standard solution to achieve a concentration of 50 ppm. The resulting solutions were then adjusted to pH=1.8 using 4 M sulfuric acid. Subsequently, 0.5 mL of the solution was mixed with 50 μL of deuterium oxide (D_2O) for the ^1H NMR measurements.

Calculation of the Faradaic efficiency (FE) and yield of NH_3

The FE of NH_3 was calculated using Eq. 1:

$$FE = (8F \times C_{NH4+-N} \times V \times 10^{-3})/(14 \times Q) \times 100\% \quad (1)$$

The yield of NH_3 was calculated using the Eq. 2:

$$\text{Yield of } NH_3 = (C_{NH4+-N} \times V \times 10^{-3})/(14 \times t \times S) \quad (2)$$

where V is the electrolyte volume in the reactor (0.05 L), C_{NH4+-N} is the concentration of ammonium measured by IC (ppm), F is the Faraday constant (96485 C mol^{-1}), t is the electrolysis time, S is the geometric area of the electrocatalyst (1 cm^2), and Q is the total charge passing through the electrode.

Density functional theory (DFT) calculation method

All DFT calculations were performed using the Vienna *ab initio* simulation package (VASP 5.4.4).[1-3] The Perdew-Burke-Ernzerhof (PBE) function of the Generalized Gradient Approximation (GGA) is used to describe the exchange-correlation energy.[4] To describe the expansion of the electronic eigenfunctions, the projector-augmented wave (PAW) method was applied with a kinetic energy cutoff of 500 eV.[5,6] The total energy and force convergence threshold were set to 10^{-4} eV and 0.02 eV $Å^{-1}$, respectively. The (311) facet of Co_3O_4 was the dominant facet identified in XRD and TEM characterization studies. Therefore, a Co_3O_4(311) surface model was built, and a 2 × 2 supercell used as the model system. To simulate the role of BCDs in the BCDs/Co_3O_4/CC catalyst, a graphene layer with B doping was built on the Co_3O_4 surface. The Brillouin zone was sampled with a 2 × 2 × 1 k-point grid of the Monkhorst-Pack scheme.[7] The van der Waals interactions were considered using the empirical correction via the DFT+D3 scheme.[8,9]

The adsorption energy E_{ads} is defined as:

$$E_{ads} = E_{adsorbates/slab} - E_{adsorbates} - E_{slab} \quad (1)$$

where $E_{absorbates/slab}$, $E_{adsorbates}$ and E_{slab} are the total energy of surface slabs with adsorbates, the free adsorbates, and the bare surface slabs of models, respectively. According to these definitions, a negative E_{ads} value indicates an exothermic adsorption process.

The calculated hydrogen electrode model is used to simulate the electrochemical reaction.[10] The Gibbs free energy change (ΔG) of each elementary step is calculated by the following formula:

$$\Delta G = \Delta E + \Delta E_{ZPE} - T\Delta S + \Delta G_{pH} + \Delta G_U \qquad (2)$$

Where ΔE is the reaction energy that can be directly obtained by the total energies of DFT. ΔE_{ZPE} and ΔS are the difference in zero-point energy and entropy between the products and the reactants at room temperature (T = 298.15 K), respectively. The difference in zero-point energy could be calculated from the vibration frequency. The entropy and vibrational frequencies of free molecules (such as H_2, and NH_3) were taken from the NIST database. The effect of the applied electrode potential and pH are contained by the correction of ΔG_U and ΔG_{pH}, respectively.

Figures

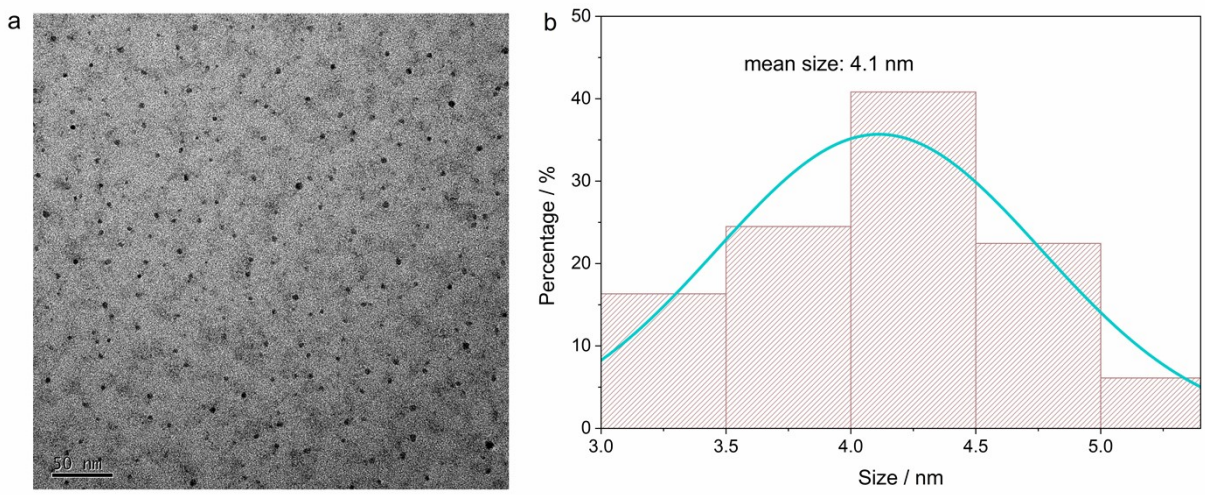

Figure S1. (a) The TEM image and (b) size distribution diagram of BCDs.

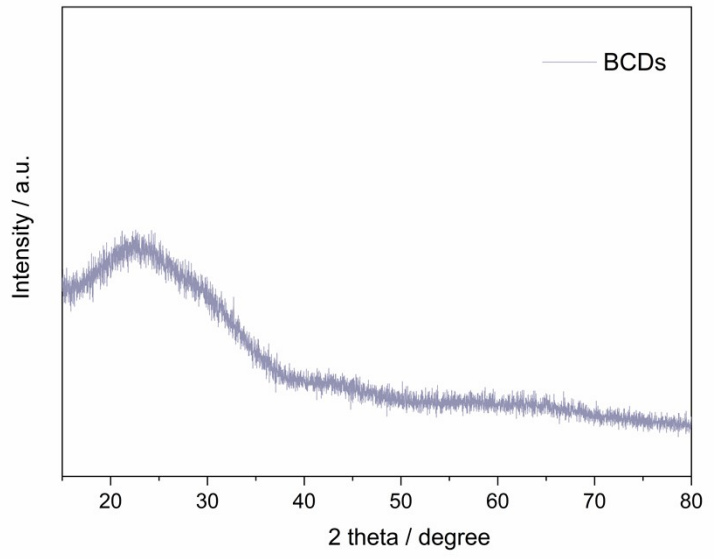

Figure S2. The XRD spectrum of BCDs.

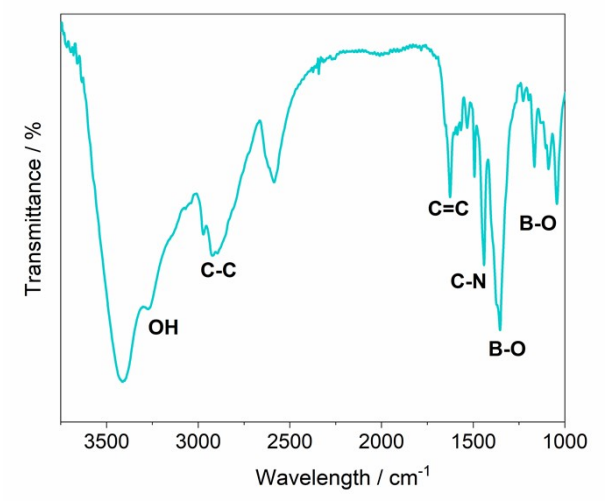

Figure S3. The Fourier transform infrared spectroscopy (FT-IR) of BCDs.

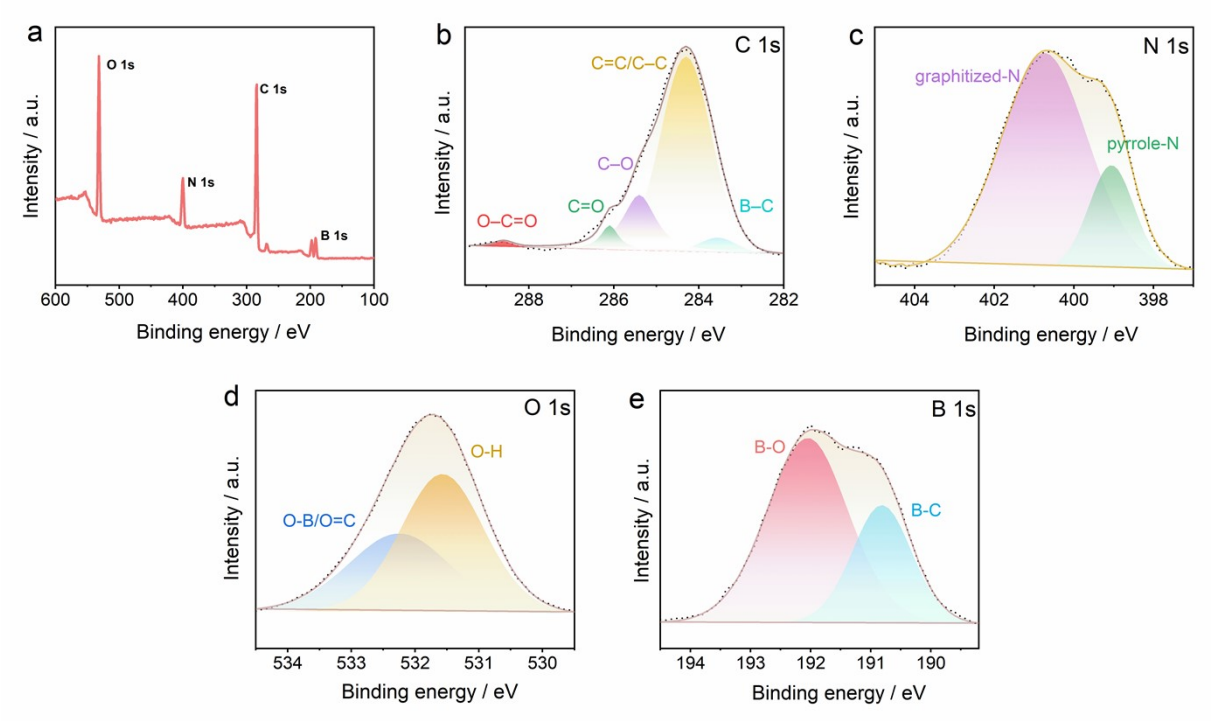

Figure S4. XPS spectra of BCDs. (a) Survey spectrum. (b) C 1s. (c) N 1s. (d) O 1s. (e) B 1s.

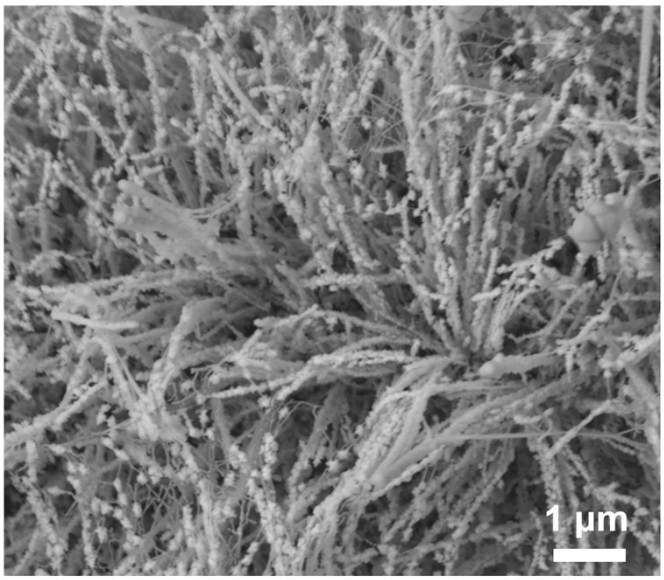

Figure S5. SEM image of Co_3O_4/CC.

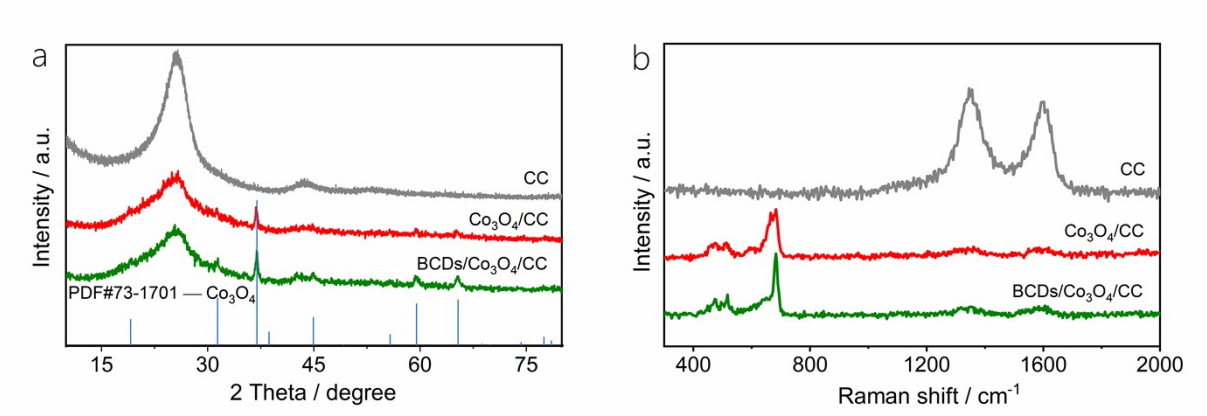

Figure S6. (a) XRD and (b) Raman spectra of BCDs/Co_3O_4/CC, Co_3O_4/CC and CC.

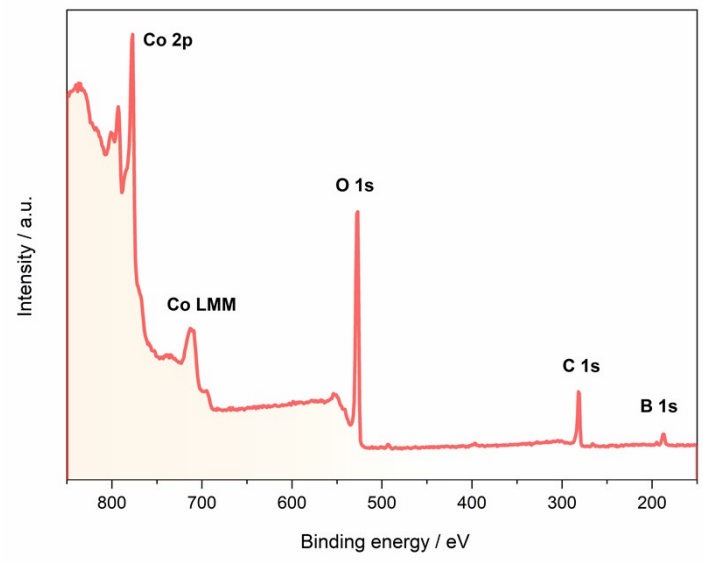

Figure S7. XPS survey spectrum of BCDs/Co_3O_4/CC.

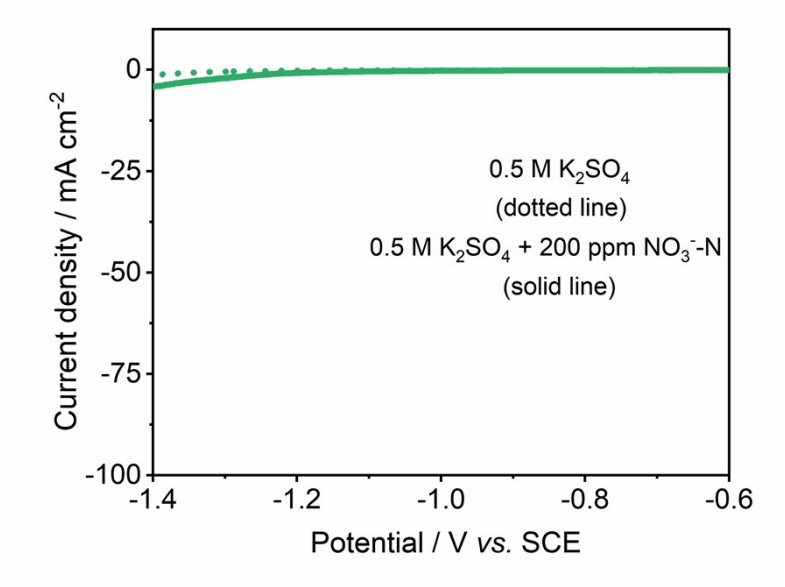

Figure R8. LSV curves of BCDs/CC collected in a 0.5 M K_2SO_4 electrolyte (dotted line) and a 0.5 M K_2SO_4 + 200 ppm NO_3^--N electrolyte (solid line).

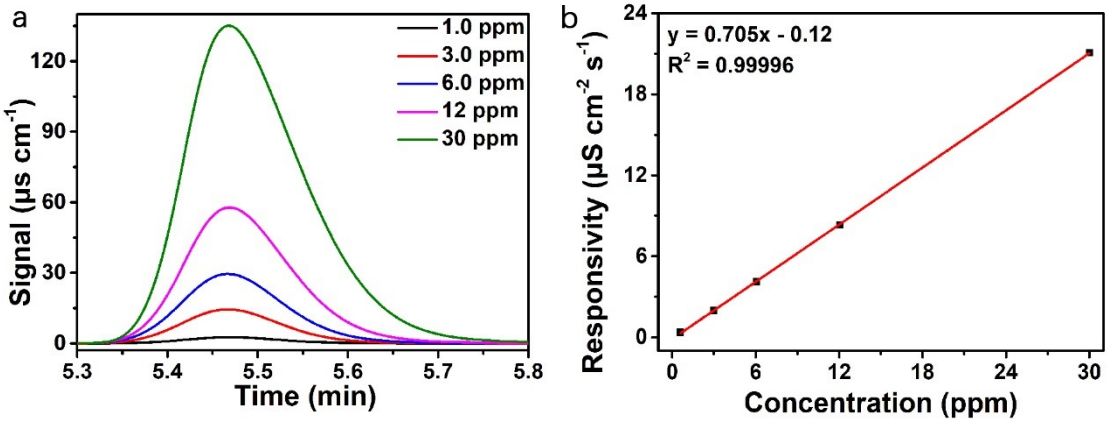

Figure S9. IC standard curves of NO_3^--N. (a) IC spectra for KNO_3 solutions with different NO_3^--N concentrations. (b) Calibration curve of NO_3^--N.

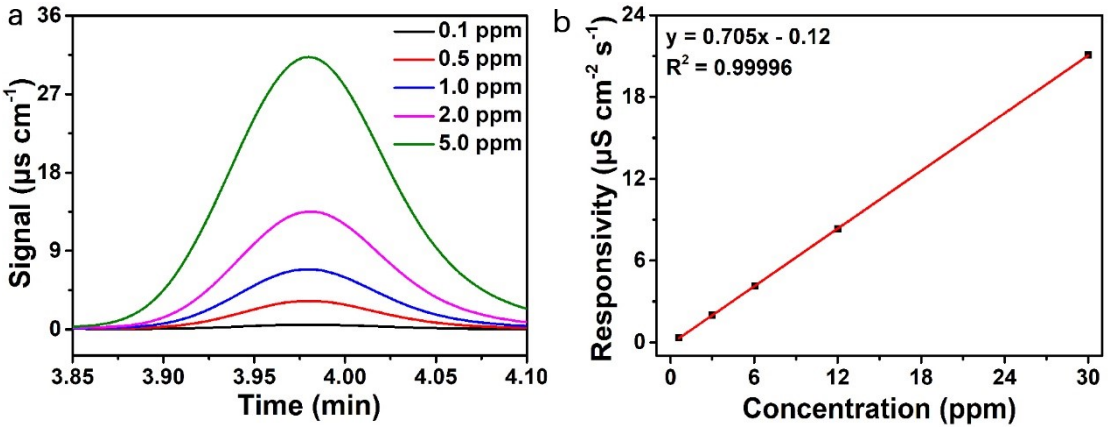

Figure S10. IC standard curves of NO_2^--N. (a) IC spectra for KNO_2 solutions with different NO_2^--N concentrations. (b) Calibration curve of NO_2^--N.

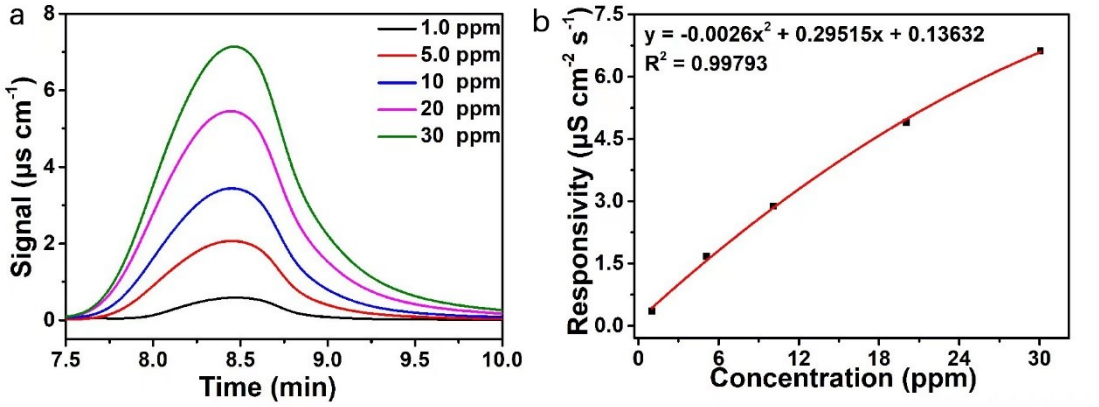

Figure S11. IC standard curves of NH_4^+-N. (a) IC spectra for NH_4Cl solutions with different NH_4^+-N concentrations. (b) Calibration curve of NH_4^+-N.

References

[1] Kresse G., Hafner J. Ab initio molecular dynamics for liquid metals. *Phys. Rev. B*, **1993**, *47*, 558.

[2] Kresse G, Hafner J. Ab initio molecular-dynamics simulation of the liquid-metal-amorphous-semiconductor transition in germanium. *Phys. Rev. B*, **1994**, *49*, 14251.

[3] Kresse G., Furthmüller J. Efficient iterative schemes for ab initio total-energy calculations using a plane-wave basis set. *Phys. Rev. B*, **1996**, *54*, 11169.

[4] Perdew J., Burke K., Ernzerhof M. Generalized gradient approximation made simple. *Phys. Rev. Lett.*, **1996**, *77*, 3865.

[5] Blochl P. Projector augmented-wave method. *Phys. Rev. B*, **1994**, *50*, 17953.

[6] Kresse G., Joubert D. From ultrasoft pseudopotentials to the projector augmented-wave method. *Phys. Rev. B*, **1999**, *59*, 1758.

[7] Monkhorst H., Pack J. Special points for Brillouin-zone integrations. *Phys. Rev. B*, **1976**, *13*, 5188.

[8] Grimme S., Antony J., Ehrlich S., et al. A consistent and accurate ab initio parametrization of density functional dispersion correction (DFT-D) for the 94 elements H-Pu. *J. Chem. Phys*., **2010**, *132*, 154104.

[9] Grimme S., Ehrlich S., Goerigk L. Effect of the damping function in dispersion corrected density functional theory. *J. Comput. Chem.*, **2011**, *32*, 1456.

[10] Nørskov J., Rossmeisl J., Logadottir A., et al. Origin of the overpotential for oxygen reduction at a fuel-cell cathode. *J. Phys. Chem. B*, **2004**, *108*, 17886.